Metrol. Meas. Syst., Vol. 31 (2024) No. 1, pp. 115–133
DOI: 10.24425/mms.2024.148539

PAN POLSKA AKADEMIA NAUK

METROLOGY AND MEASUREMENT SYSTEMS
Index 330930, ISSN 0860-8229
www.metrology.wat.edu.pl

M&MS

PERFORMANCE EVALUATION OF THE SUSPENSION SYSTEM ON MAGLEV TRAINS BASED ON MEASUREMENT DATA

Fei Ni[1)], Yawen Dai[2)], Junqi Xu[1)], Lijun Rong[1)], Qinghua Zheng[3)]

1) National Maglev Transportation Engineering R&D Center, Tongji University, Shanghai 201804, China
(✉ *junqixu@tongji.edu.cn*)
2) Institute of Rail Transit, Tongji University, Shanghai 201804, China
3) Thyssenkrupp Transrapid GmbH, Munich 80809, Germany

Abstract

In order to ensure the safe operation of electromagnetic suspension (EMS) maglev trains, it is necessary to pay attention to the control loop performance of the suspension system. The suspension system with closed-loop control is tuned to achieve excellent performance at its early stage of operation. After running for a period of time, the control loop may encounter problems e.g., degraded operation, and paralysis may occur in severe cases. In order to quantify the control performance of the suspension system in an explicable manner, this paper proposed a data-driven control loop performance evaluation method based on fractal analysis, which does not require any external sensors and can be applied without data source restrictions such as dimension, volume and resolution. The control loop performances of such suspension systems were monitored, analysed, and evaluated by cross-sectional study, based on the field data of a commercial operation line in the commissioning stage. Furthermore, the track condition was revealed by capturing performance changes of the suspension system running on different guideway girders. The results demonstrate that the proposed method enables early warning of the degeneration of the suspension systems and the track.

Keywords: maglev train, suspension system, performance evaluation, fractal analysis, Hurst index.

1. Introduction

Among recent advancements of transportation systems, the maglev train has fast operational speed, high stability, good comfort, strong climbing ability, and environmental friendliness, thanks to the characteristics of no mechanical contact between the vehicle and the rails, and no wheel-rail adhesion. The commercial operation of the *electro-magnetic suspension* (EMS) type maglev trains requires high reliability and operating performance, since the EMS system is nonlinear and open-loop unstable, which requires active control to achieve stable suspension. As the core component of the maglev train, the suspension controller is designed to track the given values of the suspension gap within allowable range, taking into consideration of the actual gap value

Article history: August 2, 2023; revised October 20, 2023; accepted November 13, 2023; available online January 31, 2024.

fed back by the suspension gap sensor, the acceleration readings, and the current value through the electromagnet coil fed back by the current sensor. The calculated output control pulse is applied to control the on-off time of the chopper switch tube and thus adjust the coil current of the suspension electromagnet, always to keep the suspension gap close to the rated value with allowable fluctuations, to achieve stable suspension of the maglev train.

During the operation of the maglev train, the performance of the suspension control loop can be significantly affected by external disturbances and the decrease of sensor sensitivity over time, which is necessary to be evaluated to ensure the safe and stable operation. Actually, high quality transport service of the maglev train requires constant attention and close supervision to sustain excellent performance, as like the majority of industrial control loops. In 1989, Harris [1] proposed measures to apply the timing analysis tool to obtain feedback control of irrelevant quantities according to the regular operating data of the system and used it as a benchmark to evaluate the performance of the control loop, forming a new framework in the field of control loop performance monitoring. Based on his work, scholars have expanded the minimum variance benchmark and extended other forms of evaluation methods [2–5].

For the maglev train suspension system, preliminary research mainly focused on dynamic stability [6–8], running smoothness [9–11] and advanced control algorithms [12–16]. In recent years, the performance analysis and evaluation methods of suspension control systems have begun to attract special attention of researchers. Due to the complex structure and various influencing factors of the suspension control system in practice, it is difficult to establish an accurate mathematical model. However, data-driven analysis methods do not require accurate model information, and thus it is feasible to diagnose the control loop with improved measures for extracting performance metrics from the closed-loop process data of the suspension control system. Yu *et al.* [17] evaluated changes of the suspension quality under different working conditions by quantifying the fluctuation of the characteristic variables of the suspension system during train operation. Ding *et al.* [18] analysed the applicability of traditional performance evaluation methods in suspension control systems in two aspects: determinism and robustness. Song *et al.* [19] introduced two commonly used classical index systems in the field of control loop performance evaluation into the electromagnetic suspension control system for the first time and carried out the data-driven control loop performance evaluation based on the measured data. Liu *et al.* [20] proposed to establish the *autoregressive moving-average model* (ARMA) model of the suspension control system and judged the performance and working state of the control system based on the minimum variance criterion and the maglev data. Xu *et al.* [21] proposed real-time performance indicators based on data-driven stability performance monitoring and carried out real-time stability performance monitoring and evaluation of the maglev train suspension system. Liu *et al.* [22] used the fuzzy comprehensive evaluation method for integrated evaluation of the maglev train suspension system, and the feasibility of the method was verified by experiments.

The majority of the aforementioned approaches assumed Gaussian properties in the control loop of the suspension system. However, it might be inappropriate to presume that signals such as ones reflecting the suspension gap and its acceleration are subject to Gaussian distributions, which often present fat-tail or multi-peak characteristics in real applications. In contrast to the existing methods, fractal measures enable to cope with the non-Gaussian problem and lead to a broader insight into the control loop. There are several ways to depict the fractal hypothesis, and one of them is to obtain the Hurst index, which measures time series persistence and reflects the hidden long-term trends in the time series. In 1951, British hydrologist H.E. Hurst [23] proposed to analyse and estimate the Hurst index by rescaled range analysis to describe time series correlations when studying a hydrological phenomenon of the river Nile. Mandelbrot and Wallis [24] improved and developed the rescaled range method making it one of the main methods to estimate the

Hurst index. In 2002, Chen *et al.* [25] proposed to calculate the Hurst index with the detrended fluctuation method and proved the stability and reliability of the algorithm. In 2012, Srinivasan and Spinner [26] further evaluated the performance of control loops using detrended fluctuation analysis. In 2016, Das and Srinivasan [27] combined the Hurst index with the Mahalanobis distance to design a *multiple-input multiple-output* (MIMO) controller performance index for control loop performance evaluation. In 2017, Domański and Ławryńczuk [28] evaluated the control performance using a fractal measurement method that employed the concept of a *rescaled range* (R/S) plot based on Hurst index estimation. Two years later, Domański [29] investigated the robustness of fractal persistence measures to interference with different statistical properties, confirming that fractal measures can be applied as robust alternative to standard statistics. In 2021, Khosroshahi and Poshtan [30] proposed a performance evaluation index for multivariate control loops based on the Hurst index.

The challenge lies in the need for more appropriate performance evaluation metrics for suspension systems. Notably, the dynamic nature of random signals such as ones reflecting the suspension gap and its vertical acceleration during maglev train operation, which exhibit self-similarity, led us to employ fractal measures, specifically the Hurst index, as a representative metric for evaluating the performance of the suspension system's control loops. With the added complexity, fractal analysis, a powerful tool in various fields, remains underutilized in the domain of maglev transportation systems. To address this gap, our paper pioneers the application of fractal analysis for the control loop performance assessment of maglev train suspension systems.

The method introduced in this paper demonstrates innovation across several key dimensions:

1. Introduction of a data-driven control loop performance evaluation framework, leveraging fractal analysis, uniquely customized for maglev trains.
2. Emphasis on leveraging real-time data shared by the suspension control system, effectively eliminating the requirement for supplementary sensors.
3. The proposed method offers a practical solution for controller debugging before the maglev train enters commercial operation, and equally facilitates continuous post-operation controller monitoring.

The rest of this paper is organized as follows. Section 2 briefly introduces the control loop of the electromagnetic suspension system. Section 3 details the performance evaluation method, including the classical R/S analysis, the Hurst index estimation method and the comprehensive index estimation method. Then, the proposed method is validated using field data by both cross-sectional studies and longitudinal research, respectively, in Section 4. Finally, Section 5 concludes this paper.

2. Control Loop of the Electromagnetic Suspension System

To levitate an EMS maglev train, a hierarchical, modular structure is commonly adopted [31]. The module is an independent unit that integrates functions of suspension, guidance and traction based on four suspension electromagnets. Two modules form a suspension frame through the connection of anti-roll beams and several frames form the suspension system of an EMS maglev train. For instance, a five-frame EMS maglev train is equipped with 10 suspension modules and 20 sets of single-point suspension systems, as shown in Fig. 1.

The modular design realizes the mechanical decoupling between electromagnets to a feasible extent, which enables the decentralized control strategy to be conducted on the suspension system over the whole vehicle. Therefore, the design of the control loop for the overall suspension system is simplified to the design of individual controllers for each single-point electromagnet.

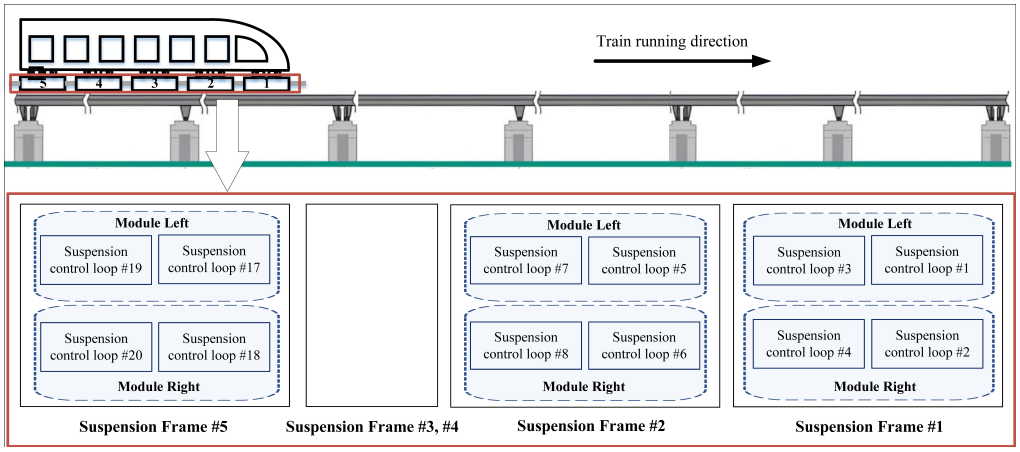

Fig. 1. Configuration of suspension systems on an EMS maglev train.

The control loop of each single-point suspension system of an EMS maglev train consists of sensors, electromagnets, a suspension controller, choppers, a power supply and other equipment. The control goal of each single-point suspension system is to keep the suspension gap within an allowable error range of the set value under the influence of various disturbances. From the perspective of running safety and ride comfort, it is expected that the suspension control loop can provide means to follow track alignment and irregularity on the track surface in form of low-frequency long-wave, while not being affected by the irregularities in form of high-frequency short wave.

Generally, a single-point suspension system is mainly composed of electromagnets, sensors, suspension controllers, choppers, and other units, of which the suspension controller is the core part of the whole system. The sensors yield the measured air gap between the electromagnet and the track, the acceleration of the electromagnet, the current of the coil winding and other signals to the controller.

The suspension sensor plays the pivotal role in the suspension control system and is primarily comprised of four integral components: a probe coil, analogue circuitry, digital circuitry and an accelerometer. Positioned at the end of the electromagnet, the suspension sensor serves the crucial function of detecting the gap between the electromagnet pole plate and the track pole surface, measuring the vertical acceleration of the electromagnet alongside. It then transmits the measurement signal to the suspension controller. Additionally, current sensors are employed to gauge the excitation current of suspension electromagnets, serving as a critical feedback parameter in the feedback control system. Based on continuously measured data from sensors, the current of the coil winding can be adjusted in time by the suspension controller to maintain an appropriate air gap, so as to realize the stable suspension of the maglev train.

3. Control Loop Performance Indices

Most of the random signal sequences in reality are non-stationary, and some of the signal have obvious self-similarity or long-correlation characteristics. Self-similarity reflects the correlation between the local and global signals and is an important feature of fractal measure, which can be described with the Hurst index.

3.1. Hurst index estimation method

3.1.1. Hurst index

In fractal analysis, if the time series y has self-similarity, it can be judged with the Hurst index [23], which is defined as follows:

$$y(k) = a^{\alpha} y\left(\frac{k}{a}\right), \tag{1}$$

where a is the scaling factor on the x-axis, a^{α} is the scaling factor on the y-axis, and α is the self-similarity parameter.

Denote the scaling factor on the x-axis and y-axis as M_x and M_y, respectively, then the self-similarity parameter α is known as the Hurst index:

$$\alpha = \frac{\ln M_y}{\ln M_x}. \tag{2}$$

3.1.2. R/S analysis

As a classical method for Hurst index estimation, the rescaled range (R/S) analysis was originally proposed by the British hydrologist H.E. Hurst [23] when undertaking the Nile dam project. Since then, the R/S analysis has been extensively used in the time series analysis, whose basic contents are as follows:

Step 1: Divide the second-order self-similar random time series $\boldsymbol{X} = \{X(1), \ldots, X(n)\}$ into K data packets with length m, and then calculate $Z_{\max}$:

$$Z_{\max} = \max\left(\sum_{i=1}^{j}\left(X_K(i) - \overline{X}_K\right)\right), \quad j = 1, 2, 3, \ldots, n, \tag{3}$$

where $Z_{\max}$ is the cumulative maximum deviation from the mean in each packet, $X_K(i)$ is the i-th data of each packet and $\overline{X_K}$ is the mean value of each packet.

Step 2: Calculate the cumulative minimum deviation from the mean value within each group:

$$Z_{\min} = \min\left(\sum_{i=1}^{j}(X_K(i) - \overline{X}_K)\right), \quad j = 1, 2, 3, \ldots, m. \tag{4}$$

The range within each group is defined as:

$$R(m) = Z_{\max} - Z_{\min}. \tag{5}$$

Step 3: Obtain the sample variance for each group by:

$$S^2(m) = \frac{1}{m-1}\sum_{i=1}^{m}(X_K(i) - \overline{X}_K)^2. \tag{6}$$

Step 4: For the sequences $\boldsymbol{X} = \{X(i), i = 1, 2, 3, \ldots, n\}$ with self-similarity, there is:

$$E\left(\frac{R(m)}{S(m)}\right) = Cm^H \tag{7}$$

where C and H are all constants. Taking logarithms on both sides of (7), the following equation can be established:

$$\log\left(E(R(m)/S(m))\right) = H\log m + \log C \tag{8}$$

Step 5: Setting $\log m$ and $\log\left(E\left(R(m)/S(m)\right)\right)$ as the x-coordinate and y-coordinate, respectively, the slope of the line α can be calculated using least squares for linear fitting.
Since $\alpha = H$, the estimate of the Hurst index is obtained as follows:

$$\alpha = \frac{\log\left(E\left(R(m)/S(m)\right)\right) - \log C}{\log m}. \tag{9}$$

3.1.3. Signal processing

The time series is often segmented to calculate the Hurst index in each period with the truncation method to study the local characteristics, but the truncation process is usually accompanied by spectrum leakage. Spectrum leakage refers to mutual influence between various spectral lines in the signal spectrum, which makes the measurement result deviate from the actual value. In order to reduce the spectral leakage, various interception functions can be used to truncate the signal, and the truncation function is called the window function, often referred to as the Hamming window [32]. The window function could be selected in consideration of signal feature and processing requirements of the analysed signal. Signal processing with the Hamming window has the advantage of small sidelobe amplitude, thus is widely used for time series analysis.

In this paper, the R/S analysis and the signal processing through the Hamming window were adopted to estimate Hurst index α.

3.2. Comprehensive index estimation method

3.2.1. Generalized Hurst index

In order to conduct the performance evaluation in the univariate case, the estimated Hurst index α was converted into a generalized Hurst index η. Under conditions where the signal is close to Gaussian white noises, the generalized Hurst index is defined as follows [26]:

$$\eta = \begin{cases} \alpha/0.5 & \text{if } \alpha \le 0.5 \\ 1.5 - \alpha & \text{if } \alpha > 0.5 \end{cases}. \tag{10}$$

In (10), the range of η is $0 \sim 1$. The closer η is to 1, the better performance of the control loop; the closer it is to 0, the worse the performance of the control loop.

3.2.2. Entropy weight method

In the case of multiple data groups with distinct features, information entropy can be used to calculate the entropy weight of each individual generalized Hurst index η, to obtain the well-founded index weights. Based on the entropy weight method [33], the comprehensive evaluation method in case of multiple indices was presented, with calculation steps for its empowerment are as follows:

Step 1: Given a group of data sets with k features $\boldsymbol{X}_1, \boldsymbol{X}_2, \ldots, \boldsymbol{X}_k$, and each data set containing n data samples $\boldsymbol{X}_i = \{X_{ij}, j = 1, 2, 3, \ldots, n\}$ $(i = 1, 2, 3, \ldots, k)$, calculate the normalized value $\boldsymbol{Y} = \{Y_{ij}, i = 1, 2, 3, \ldots, k,\ j = 1, 2, 3, \ldots, n\}$ as follows:

$$Y_{ij} = \frac{X_{ij} - \min\left(\boldsymbol{X}_i\right)}{\max\left(\boldsymbol{X}_i\right) - \min\left(\boldsymbol{X}_i\right)}, \quad (i = 1, 2, \ldots, k;\ j = 1, 2, \ldots, n). \tag{11}$$

where X_{ij} is the attribute value of the i-th feature of the j-th data sample, $\min\left(\boldsymbol{X}_i\right)$ is the minimum value of the attribute value of the i-th feature among all data samples, while $\max\left(\boldsymbol{X}_i\right)$ is the maximum value.

Step 2: Calculate the proportion of the attribute value of the jth data sample in the data set with the ith feature:

$$p_{ij} = \frac{Y_{ij}}{\sum_{i=1}^{k} Y_{ij}}, \quad (i = 1, 2, \ldots, k;\ j = 1, 2, \ldots, n). \tag{12}$$

If $p_{ij} = 0$, then the following equation satisfies:

$$\lim_{p_{ij} \to 0} p_{ij} \ln p_{ij} = 0. \tag{13}$$

Step 3: Get the information entropy of each feature as follows:

$$E_i = -\frac{1}{\ln n} \sum_{j=1}^{n} p_{ij} \ln p_{ij},\ (i = 1, 2, \ldots, k). \tag{14}$$

Step 4: Calculate the weight for each feature according to information entropy:

$$W_i = \frac{1 - E_i}{k - \sum_{i=1}^{k} E_i},\ (i = 1, 2, \ldots, k), \tag{15}$$

where sum of the weight vector of the extracted n-dimensional feature index $\boldsymbol{W} = \{W_i, i = 1, 2, 3, \ldots, k\}$ is equal to 1.

Step 5: According to the weight in (15), finally obtain the comprehensive index:

$$\gamma_i = \sum_{i=1}^{k} w_i \eta_i, \tag{16}$$

where η_i $(i = 1, 2, 3, \ldots, k)$ is the generalized Hurst index corresponding to the i-th feature.

4. Performance Evaluation Based on the Comprehensive Index

In Section 3, estimation methods for the Hurst index and the comprehensive index were introduced. In this section, the proposed method will be applied to implement the control loop performance evaluation of the electromagnetic suspension system.

4.1. Data acquisition and pre-processing

Based on the data collected from a commercial maglev line in the commissioning stage, the performance evaluation method was tested and validated in a real-world application. In this paper, the object of study is a five-frame low-speed EMS maglev train with 20 single-point suspension systems, as shown in Fig. 2. There are 20 control loops corresponding to 20 single-point suspension systems over the whole car, denoted as #1 ~ #20.

The chosen model for the suspension sensors is CF-ZJ-SZ-03B, characterized by a rated measurement gap of 8 mm and a measurement range spanning from 0 mm to 20 mm. Within this range, the maximum output error is ±0.2 mm, and the resolution is 60 μm. In terms of acceleration measurement, the range extends from –5 g to +5 g, with a maximum error of ±0.125 g and

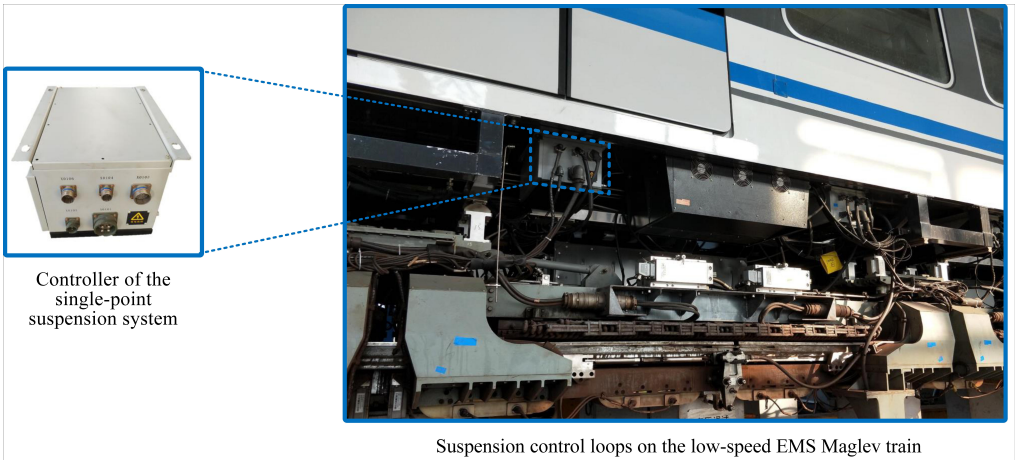

Fig. 2. Visual representation of suspension control loop on the low-speed EMS maglev train.

a resolution of 0.05 g within this range. Fig. 3 provides an illustration of the suspension sensor. The current sensor model in use is LA 205-S/SP1, with a primary nominal current rating of 200 A. The primary current measurement range spans from 0 A to ±300 A, featuring a linearity error of less than 0.1%. Additionally, it offers an operational temperature range from –10°C to +85°C.

Fig. 3. A visual representation of the suspension sensor.

The sensors used in each control loop have sampling frequency 1 kHz, however, data at 10 Hz were logged to save storage space. The measurement quantities, including air gap, current and acceleration, were recorded for 2800 s to evaluate the control loop performance herein. It is worth noting that every control loop encompasses a significant amount of uncertainty, which mainly include sensor accuracy, modelling mismatch, external disturbances, dynamic variations, communication delays and component variability. During the operation of the train, the characteristics of these sources of uncertainty are integrated into the on-site measurement data.

Taking suspension Control Loop #15 for illustration, time series of measurement data are shown in Fig. 4.

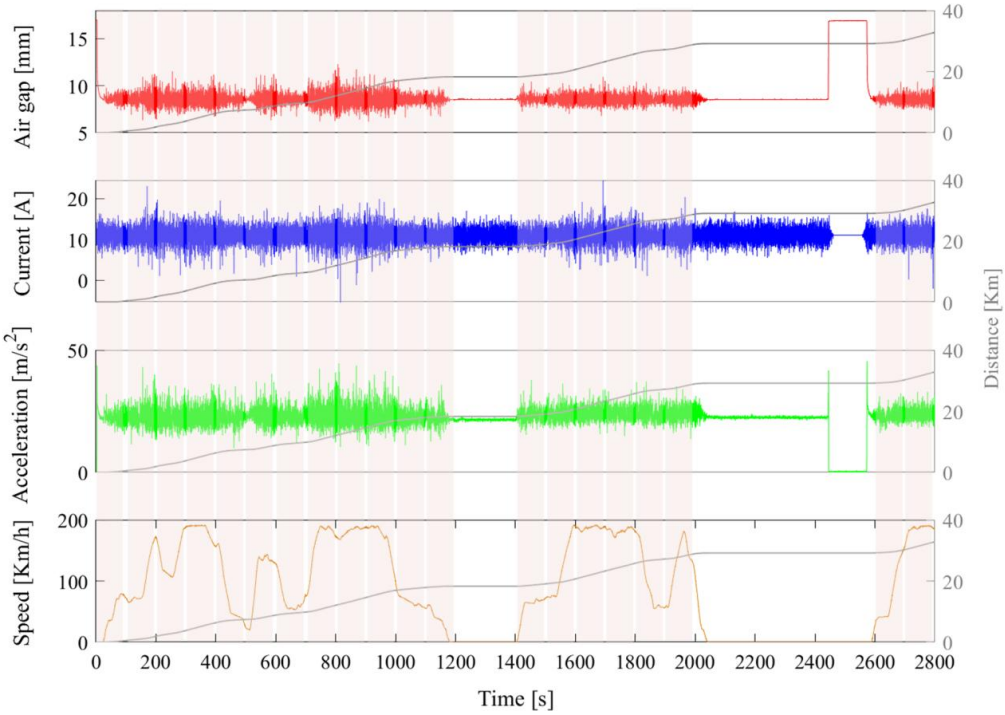

Fig. 4. Operation status of the suspension system corresponding to Control Loop #15.

In Fig. 4, the right axis represents the distance from the starting point. It is found that the maglev train experienced several working conditions during the timespan such as acceleration, deceleration, and standstill. For clarity, the time intervals when the maglev train speed was 0 Km/h were ignored. To gain an insight into the influence of working conditions on the control loop performance, the total duration of 2800s is segmented into 20 equal intervals that are denoted as t1~t20. The duration of each period of time is 100s, for instance, t1 and t2 refers to [0.1 s, 100.0 s] and [100.1 s, 200.0 s], respectively.

4.2. Performance evaluation of single control loop in multiple time periods

With regard to Control Loop #15, the *probability density functions* (PDFs) of the air gap, current, and acceleration signals in the 20 time periods can be smoothed by using *kernel density estimation* (KDE), which are displayed in Fig. 5. According to Fig. 5a and 5b, the shape of the PDF in t12 is steeper than that in other time periods.

As to the obtained PDFs in Fig. 5, the corresponding kurtoses are calculated, as listed in Table 1. In Table 1, the kurtoses of distribution curves of the air gap signal in t12, the current signal in t2 and the acceleration signal in t9 are larger than the others.

In order to capture the changes in the real-time suspension state, the collected data were estimated with the generalized Hurst index, in addition to evaluating the performance of the control loop from the perspective of kurtosis. Based on the generalized Hurst index estimates and the related weights, the comprehensive index estimate in each time period is obtained, as listed in Table 2.

According to Table 2, it can be found that the comprehensive index estimates in the time periods t12, t1, t20 and t16 are comparatively larger, which indicates that the control loop performances in these time periods are satisfactory, and the control loop performance in the 12th period is the best. On the contrary, the comprehensive index estimates in t3, t10, t18 and t2 are comparatively small, indicating that the control loop performances in these time periods are worse.

In order to visualize the evaluation results above, the comprehensive indices of Control Loop #15 in 20 time periods are illustrated as the colour contour alongside the track beam in Fig. 6. The darker colour indicates the larger comprehensive index, *i.e.*, a superior performance of the suspension control loop. It can be found that the performance of Control Loop #15 in s12 is superior, while inferior performance occurs in s3.

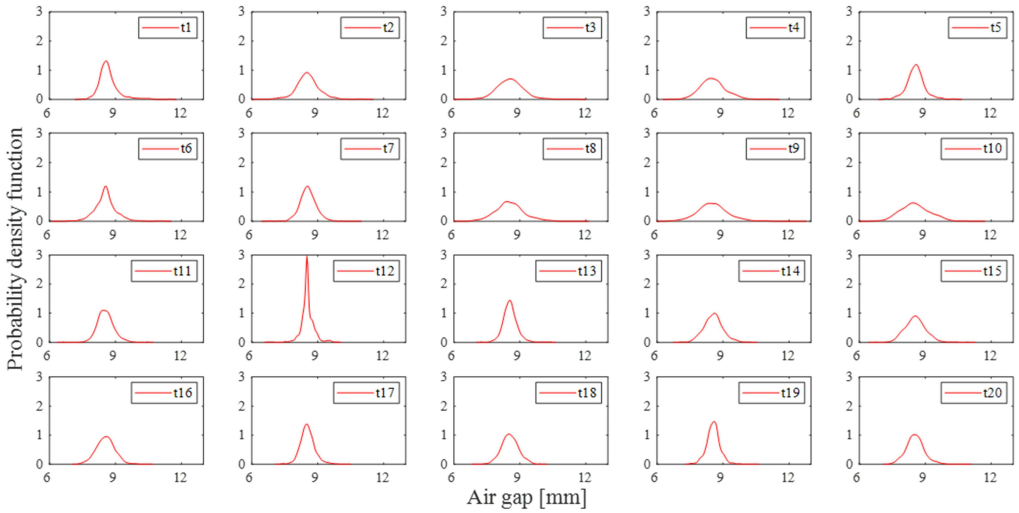

(a)

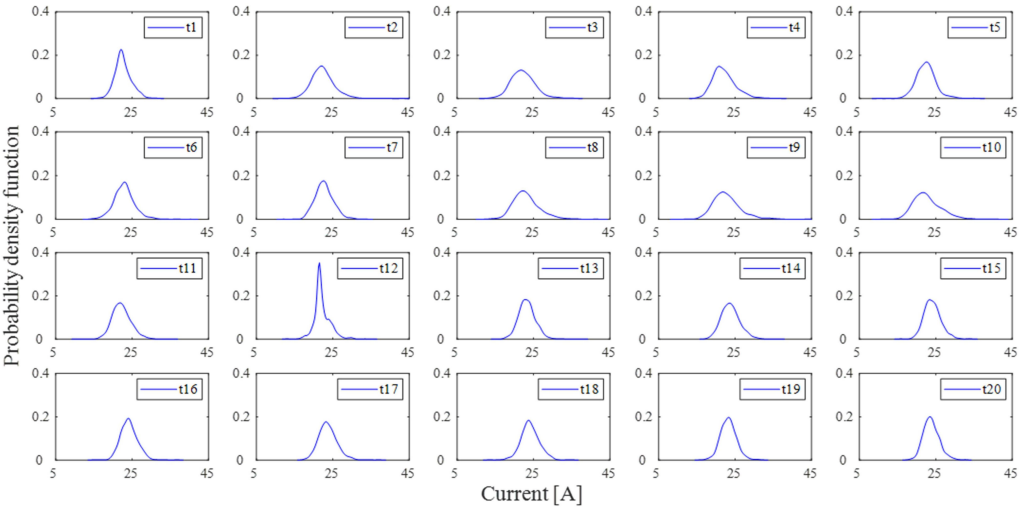

(b)

Metrol. Meas. Syst., Vol. 31 (2024), No. 1, pp. 115–133
DOI: 10.24425/mms.2024.148539

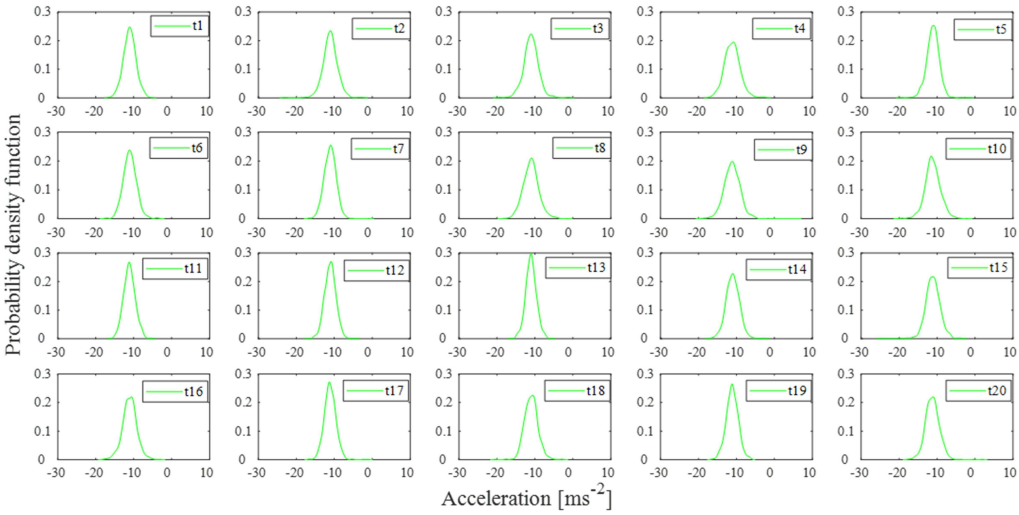

(c)

Fig. 5. PDFs of three signals in Control Loop #15. (a) air gap; (b) current; (c) acceleration.

Table 1. Kurtoses of the distribution curves of three signals of Control Loop #15.

Time interval	**t1**	**t2**	**t3**	**t4**	**t5**	**t6**	**t7**	**t8**	**t9**	**t10**
Air gap	7.90	5.74	4.27	3.84	4.95	6.45	5.54	4.32	4.91	3.35
Current	3.84	7.11	4.20	4.36	5.64	6.26	4.08	5.06	6.23	4.85
Acceleration	3.16	5.32	4.96	3.88	5.43	4.09	4.70	3.85	7.61	4.26
Time interval	**t11**	**t12**	**t13**	**t14**	**t15**	**t16**	**t17**	**t18**	**t19**	**t20**
Air gap	4.46	8.80	5.68	3.40	3.95	3.46	4.96	3.31	5.20	4.38
Current	4.11	6.84	5.17	3.74	4.31	4.37	4.43	3.95	3.86	3.79
Acceleration	3.17	3.58	3.37	4.27	6.14	3.90	5.75	4.66	3.28	6.52

Table 2. Comprehensive index estimations of Control Loop #15 in 20 time periods.

Time interval	**t1**	**t2**	**t3**	**t4**	**t5**	**t6**	**t7**	**t8**	**t9**	**t10**
γ	0.449	0.414	0.408	0.424	0.432	0.426	0.427	0.424	0.426	0.412
Time interval	**t11**	**t12**	**t13**	**t14**	**t15**	**t16**	**t17**	**t18**	**t19**	**t20**
γ	0.421	0.469	0.425	0.423	0.435	0.441	0.414	0.412	0.429	0.441

4.3. Performance evaluation of multiple control loops in single time periods

To investigate the performances among different control loops, the differences in the aspect of the generalized Hurst index can be visually represented by radar charts. Taking 20 control loops in t6 for illustration, the estimated generalized Hurst indices for the air gap, current and acceleration

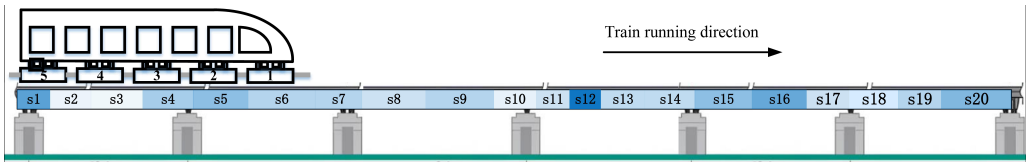

Fig. 6. Illustration of performances of Control Loop #15 in 20 sections based on the comprehensive index estimation.

signals, denoted by η_s, η_i and η_a, are displayed in the graphical format, as shown in Fig. 7. It is found that the estimated generalized Hurst indices of current and acceleration signals of the control loops within Suspension Frame #1 are the largest, whereas those within Suspension Frame #5 are the smallest. Moreover, the total of five suspension frames that is composed of four suspension control loops behave differently in the aspect of equilibrium level.

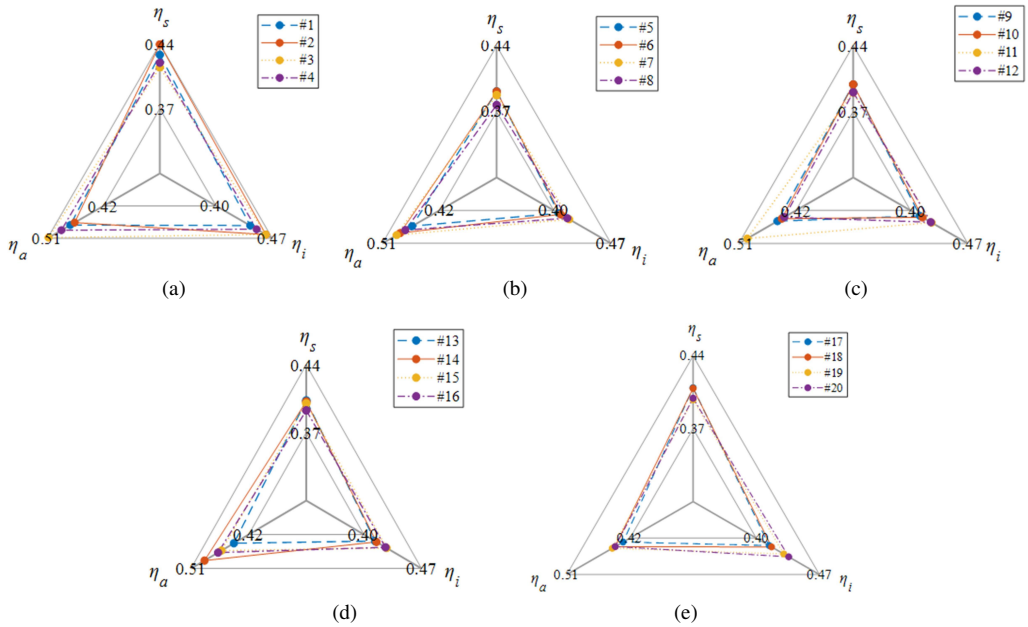

Fig. 7. Generalized Hurst index estimation of the three signals in different control loops. (a) Suspension Frame #1; (b) Suspension Frame #2; (c) Suspension Frame #3; (d) Suspension Frame #4; (e) Suspension Frame #5.

In addition to the generalized Hurst index estimation of the three signals, the relevant weight of each index can be obtained with the entropy method, whereupon the estimations of the comprehensive index for the total of 20 control loops in a certain period are obtained. In Fig. 8, the result is displayed in form of the heatmap, in which the specific comprehensive index estimation of each suspension control loop was marked with colour gradient.

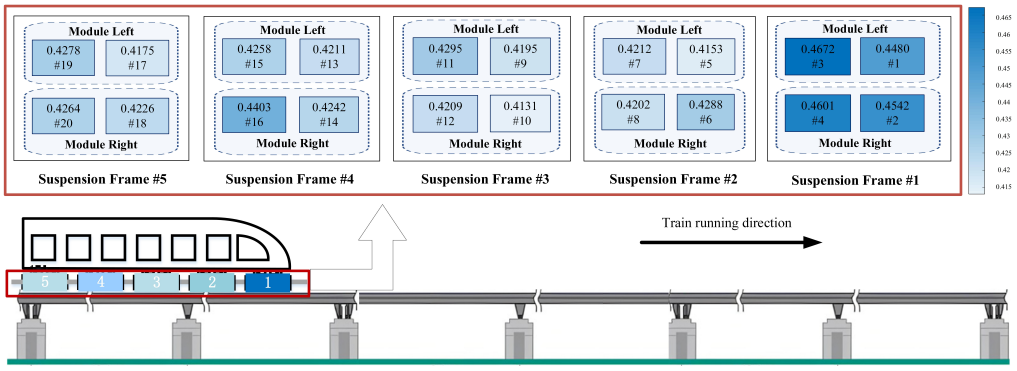

Fig. 8. Illustration of the comprehensive index estimations for 20 control loops during t6.

In Fig. 8, it can be found that the comprehensive index estimations of Control Loops #3, #2, #4 and #1 are relatively large, namely, the performances of these suspension control loops are better, which are consistent with the results obtained above. The estimated values of the comprehensive index of Control Loops #9, #13, #10 and #17 are relatively small, which indicates that these suspension control loops have relatively poor performances. Comparatively, it is concluded that the control loop performance of Suspension Frame #1 is the best while the control loops within Suspension Frame #5 have the worst performances in a single time period t6.

In like manner, the performance evaluation of multiple control loops during the other single time periods could be implemented.

4.4. Performance evaluation of multiple control loops in multiple time periods

To evaluate the performance of the suspension system and the condition of the track beam across the board, indices of 20 control loops in 20 time periods are discussed as well. Based on the air gap, current and acceleration signals of the total of 20 control loops, the generalized Hurst indices are estimated. Further, the weights of estimated values of the generalized Hurst index of the air gap, current and acceleration signals can be obtained using the entropy weight method. Afterwards, the estimated values of the comprehensive index of 20 suspension control loops in 20 time periods are calculated, which is shown in Fig. 9a. The x-axis is the time period, and the y-axis represents the numbering of the control loops.

Based on the individual index in Fig. 9a, the average value and standard deviation of the comprehensive index estimation of each control loop over the 20 time periods are calculated, as shown in Fig. 9b. As can be seen from Fig. 9b, the mean value corresponding to Control Loop #16 is the largest while that of Control Loop #10 is the smallest, which indicates that the performance of Control Loop #16 is the best and the performance of Control Loop #10 is the worst. The standard deviation corresponding to Control Loop #16 is the smallest while that of Control Loop #10 is the largest, which indicates that Control Loop #16 in 20 time periods achieves consistency in performance, whereas the performance of Control Loop #10 varies largely.

Moreover, the performance of a suspension frame can be evaluated by counting the average value and standard deviation of mean values of the related four control loops, denoted by *MM and SM*. For instance, the *MM* for Suspension Frame #1 is calculated by averaging mean values of performance indices for Control Loops #1, #2, #3, and #4; the *SM* for Suspension Frame #1 is calculated by calculating the standard deviation of mean values of performance indices for Control Loops #1, #2, #3, and #4. Likewise, performance of the suspension frame can be also evaluated by counting the average value of standard deviations of the related four control loops, denoted by *MS*. For example, the *MS* for Suspension Frame #1 is calculated by averaging standard deviations of performance indices for Control Loops #1, #2, #3, and #4. The three groups of statistical value, *i.e.*, *MM*, *SM and MS*, are listed according to different suspension frames, as shown in Fig. 9c.

It can be seen from Fig. 9c that the *MM* of Suspension Frame #1 is the largest and the *MM* of Suspension Frame #5 is the smallest, which reveals that the performance of Suspension Frame #1 is the best while that for Suspension Frame #5 is the worst. The *SM* of Suspension Frame #4 is the largest, and the *SM* of Suspension Frame #5 is the smallest, which shows that the inconsistency of the control loop performances for Suspension Frame #4 is the largest, and that for Suspension Frame #5 is the smallest. The *MS* of Suspension Frame #5 is the largest and the *MS* of Suspension Frame #2 is the smallest, which reveals that control loops for Suspension Frame #5 represent the largest performance difference in each period, whereas performances of control loops for Suspension Frame #2 in each period are not much different.

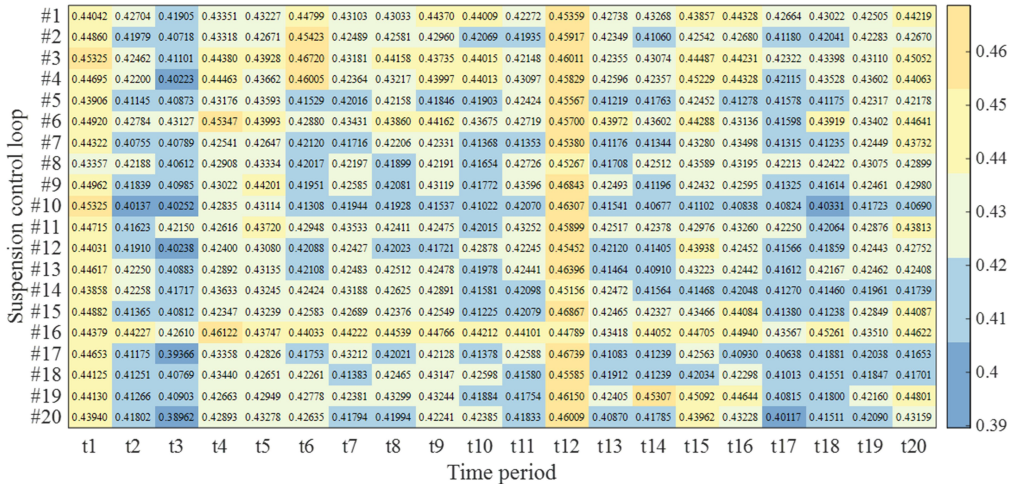
Suspension control loop
#1 0.44042 0.42704 0.41905 0.43351 0.43227 0.44799 0.43103 0.43033 0.44370 0.44009 0.42272 0.45359 0.42738 0.43268 0.43857 0.44328 0.42664 0.43022 0.42505 0.44219
#2 0.44860 0.41979 0.40718 0.43318 0.42671 0.45423 0.42489 0.42581 0.42960 0.42069 0.41935 0.45917 0.42349 0.41060 0.42542 0.42680 0.41180 0.42041 0.42283 0.42670
#3 0.45325 0.42462 0.41101 0.44380 0.43928 0.46720 0.43181 0.44158 0.43735 0.44015 0.42148 0.46011 0.42355 0.43074 0.44487 0.44231 0.42322 0.43398 0.43110 0.45052
#4 0.44695 0.42200 0.40223 0.44463 0.43662 0.46005 0.42364 0.43217 0.43997 0.44013 0.43097 0.45829 0.42596 0.42357 0.45229 0.44328 0.42115 0.43528 0.43602 0.44063
#5 0.43906 0.41145 0.40873 0.43176 0.43593 0.41529 0.42016 0.42158 0.41846 0.41903 0.42424 0.45567 0.41219 0.41763 0.42452 0.41278 0.41578 0.41175 0.42317 0.42178
#6 0.44920 0.42784 0.43127 0.45347 0.43993 0.42880 0.43431 0.43860 0.44162 0.43675 0.42719 0.45700 0.43972 0.43602 0.44288 0.43136 0.41598 0.43919 0.43402 0.44641
#7 0.44322 0.40755 0.40789 0.42541 0.42647 0.42120 0.41716 0.42206 0.42331 0.41368 0.41353 0.45380 0.41176 0.41344 0.43280 0.43498 0.41315 0.41235 0.42449 0.43732
#8 0.43357 0.42188 0.40612 0.42908 0.43334 0.42017 0.42197 0.41899 0.42191 0.41654 0.42726 0.45267 0.41708 0.42512 0.43589 0.43195 0.42213 0.42422 0.43075 0.42899
#9 0.44962 0.41839 0.40985 0.43022 0.44201 0.41951 0.42585 0.42081 0.43119 0.41772 0.43596 0.46843 0.42493 0.41196 0.42432 0.42595 0.41325 0.41614 0.42461 0.42980
#10 0.45325 0.40137 0.40252 0.42835 0.43114 0.41308 0.41944 0.41928 0.41537 0.41022 0.42070 0.46307 0.41541 0.40677 0.41102 0.40838 0.40824 0.40331 0.41723 0.40690
#11 0.44715 0.41623 0.42150 0.42616 0.43720 0.42948 0.43533 0.42411 0.42475 0.42015 0.43252 0.45899 0.42517 0.42378 0.42976 0.43260 0.42250 0.42064 0.42876 0.43813
#12 0.44031 0.41910 0.40238 0.42400 0.43080 0.42088 0.42427 0.42023 0.41721 0.42878 0.42245 0.45452 0.42120 0.41405 0.43938 0.42452 0.41566 0.41859 0.42443 0.42752
#13 0.44617 0.42250 0.40883 0.42892 0.43135 0.42108 0.42483 0.42512 0.42478 0.41978 0.42441 0.46396 0.41464 0.40910 0.43223 0.42442 0.41612 0.42167 0.42462 0.42408
#14 0.43858 0.42258 0.41717 0.43633 0.43245 0.42424 0.43188 0.42625 0.42891 0.41581 0.42098 0.45156 0.42472 0.41564 0.41468 0.42048 0.41270 0.41460 0.41961 0.41739
#15 0.44882 0.41365 0.40812 0.42347 0.43239 0.42583 0.42689 0.42376 0.42549 0.41225 0.42079 0.46867 0.42465 0.42327 0.43466 0.44084 0.41380 0.41238 0.42849 0.44087
#16 0.44379 0.44227 0.42610 0.46122 0.43747 0.44033 0.44222 0.44539 0.44766 0.44212 0.44101 0.44789 0.43418 0.44052 0.44705 0.44940 0.43567 0.45261 0.43510 0.44622
#17 0.44653 0.41175 0.39366 0.43358 0.42826 0.41753 0.43212 0.42021 0.42128 0.41378 0.42588 0.46739 0.41083 0.41239 0.42563 0.40930 0.40638 0.41881 0.42038 0.41653
#18 0.44125 0.41251 0.40769 0.43440 0.42651 0.42261 0.41383 0.42465 0.43147 0.42598 0.41580 0.45585 0.41912 0.41239 0.42034 0.42298 0.41013 0.41551 0.41847 0.41701
#19 0.44130 0.41266 0.40903 0.42663 0.42949 0.42778 0.42381 0.43299 0.43244 0.41884 0.41754 0.46150 0.42405 0.45307 0.45092 0.44644 0.40815 0.41800 0.42160 0.44801
#20 0.43940 0.41802 0.38962 0.42893 0.43278 0.42635 0.41794 0.41994 0.42241 0.42385 0.41833 0.46009 0.40870 0.41785 0.43962 0.43228 0.40117 0.41511 0.42090 0.43159
t1 t2 t3 t4 t5 t6 t7 t8 t9 t10 t11 t12 t13 t14 t15 t16 t17 t18 t19 t20
Time period
0.46 0.45 0.44 0.43 0.42 0.41 0.4 0.39

(a)

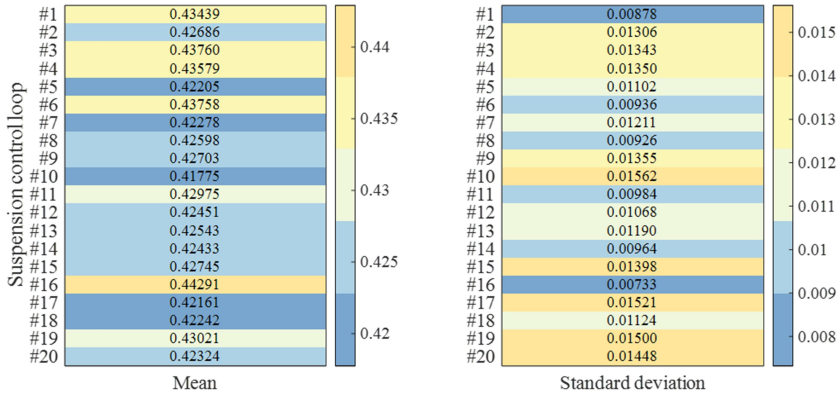
Suspension control loop
#1 0.43439
#2 0.42686
#3 0.43760
#4 0.43579
#5 0.42205
#6 0.43758
#7 0.42278
#8 0.42598
#9 0.42703
#10 0.41775
#11 0.42975
#12 0.42451
#13 0.42543
#14 0.42433
#15 0.42745
#16 0.44291
#17 0.42161
#18 0.42242
#19 0.43021
#20 0.42324
0.44 0.435 0.43 0.425 0.42
Mean
#1 0.00878
#2 0.01306
#3 0.01343
#4 0.01350
#5 0.01102
#6 0.00936
#7 0.01211
#8 0.00926
#9 0.01355
#10 0.01562
#11 0.00984
#12 0.01068
#13 0.01190
#14 0.00964
#15 0.01398
#16 0.00733
#17 0.01521
#18 0.01124
#19 0.01500
#20 0.01448
0.015 0.014 0.013 0.012 0.011 0.01 0.009 0.008
Standard deviation

(b)

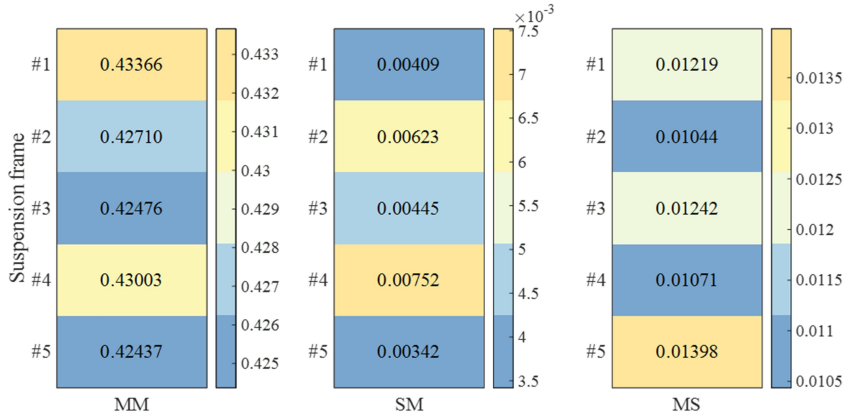
Suspension frame
#1 0.43366
#2 0.42710
#3 0.42476
#4 0.43003
#5 0.42437
0.433 0.432 0.431 0.43 0.429 0.428 0.427 0.426 0.425
MM
×10-3
#1 0.00409
#2 0.00623
#3 0.00445
#4 0.00752
#5 0.00342
7.5 7 6.5 6 5.5 5 4.5 4 3.5
SM
#1 0.01219
#2 0.01044
#3 0.01242
#4 0.01071
#5 0.01398
0.0135 0.013 0.0125 0.012 0.0115 0.011 0.0105
MS

(c)

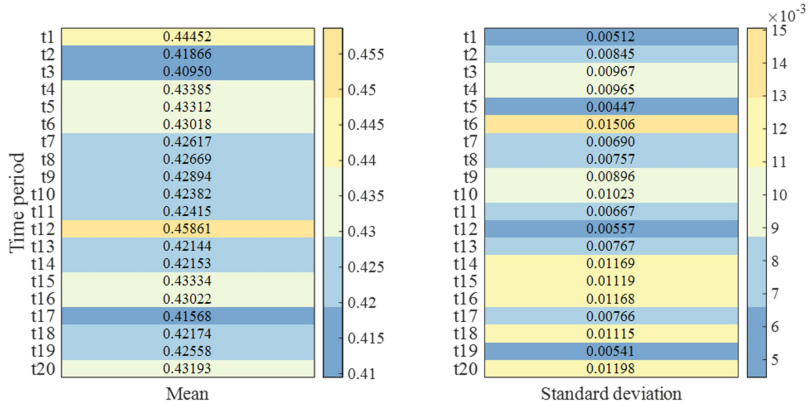

(d)

Fig. 9. Heatmaps of the estimated comprehensive indices and statistical values. (a) 20 control loops in 20 time periods; (b) control loops; (c) suspension frames; (d) time periods.

Taken together, it can be concluded that performances of the control loops for Suspension Frame #5 are inferior to the others which requires further analysis, in view of the same running speed and track condition. In addition, detailed statistical analysis of individual indices in Fig. 9a can be performed from another perspective. Specifically, the mean and standard deviation of comprehensive index estimations for each time period are obtained, as shown in Fig. 9d.

According to Fig. 9d, the mean value of control loops in t12 is the largest, and the mean value of control loops in t3 is the smallest, which demonstrates that the average control loop performance in t12 is the best, and that in t3 is the worst. The standard deviation of control loops in t5 is the smallest, and the standard deviation of control loops in t6 is the largest, which indicates that performances of the total of 20 control loops in t5 are not much different, and that in t6 has the largest variation. Since the average performance of over 20 control loops in t3 is the worst, factors such as the track condition in the 3rd time period need to be further analysed.

4.5. Comparative analysis of performance evaluation methods

According to the fuzzy comprehensive evaluation method [24], the evaluation result vectors are obtained from the data of Control Loops # 10 and # 16 in Sections t1–t12, as shown below:

$$\begin{aligned} \omega_{\#10} &= [0.8208, 0.0683, 0, 0.1109] \\ \omega_{\#16} &= [0.6340, 0.2551, 0, 0.1109]. \end{aligned} \tag{17}$$

The evaluation results calculated with the fuzzy comprehensive evaluation method are uniformly marked as “excellent”, aligning with the trend observed through the fractal analysis. Nevertheless, the application of the fractal analysis method reveals that Control Loop #10 outperforms Control Loop #16, providing a more distinct quantitative evaluation of various control loops. Furthermore, as the fractal analysis method operates independently of a weight matrix, the resulting evaluations maintain a relatively high level of objectivity.

5. Conclusions

In this paper, fractal analysis was introduced to evaluate the control loop performance of the electromagnetic suspension system on maglev trains. Firstly, the structure of suspension control loops, and the classic estimation methods of the Hurst index, and the R/S analysis method were briefly introduced. Next, the estimated value of the Hurst index was converted into a generalized Hurst index, to evaluate the control loop performance for each unidimensional feature. Subsequently, a comprehensive index was presented to evaluate the performance by properly weighting multiple generalized Hurst indices. At last, the effectivity of the proposed method was verified in a real-world case study based on the field data of a commercial operation line in the commissioning stage.

To sum up, the proposed method has been proved to make the risk of the degeneration of the suspension system and track tangible by resorting to early-warning tactics, thus has good practical application values. The effectiveness of this method is intricately tied to the selection of the time period's size, making the ongoing exploration of optimal time period size selection a critical challenge.

Acknowledgements

The authors gratefully acknowledge the financial support from the Natural Science Foundation of Shanghai (21ZR1466900) and the National Natural Science Foundation of China (52232013).

References

[1] Harris, T. J. (1989). Assessment of control loop performance. *Canadian Journal of Chemical Engineering*, *67*(5), 856–861. https://doi.org/10.1002/cjce.5450670519

[2] Kamrunnahar, M., Fisher, D. G., & Huang, B. (2004). Performance assessment and robustness analysis using an ARMarkov approach. *Journal of Process Control*, *14*(8), 915–925. https://doi.org/10.1016/j.jprocont.2003.12.009

[3] Liu, C., Huang, B., & Wang, Q. (2011). Control performance assessment subject to multi-objective user-specified performance characteristics. *IEEE Transactions on Control Systems Technology*, *19*(3), 682–691. https://doi.org/10.1109/TCST.2010.2051669

[4] Domański, P. D. (2018). Statistical measures for proportional-integral-derivative control quality: Simulations and industrial data. *Proceedings of the Institution of Mechanical Engineers, Part I: Journal of Systems and Control Engineering*, *232*(4), 428–441. https://doi.org/10.1177/0959651817754034

[5] Wang, J., & Zhao, C. (2021). A probabilistic framework with concurrent analytics of Gaussian process regression and classification for multivariate control performance assessment. *Journal of Process Control*, *101*, 78–92. https://doi.org/10.1016/j.jprocont.2021.03.007

[6] Rote, D. M., & Cai, Y. G. (2002). Review of dynamic stability of repulsive-force maglev suspension systems. *IEEE Transactions on Magnetics*, *38*(2), 1383–1390. https://doi.org/10.1109/20.996030

[7] Xiao, J. Z., Jian, J. W., & Zhou, Y. H. (2005). Effect of spring non-linearity on dynamic stability of a controlled maglev vehicle and its guideway system. *Journal of Sound and Vibration*, *279*(1-2), 201–215. https://doi.org/10.1016/j.jsv.2003.10.025

[8] Zhang, L., Huang, L., & Zhang, Z. (2009). Stability and Hopf bifurcation of the maglev system with delayed position and speed feedback control. *Nonlinear Dynamics*, *57*(1-2), 197–207. https://doi.org/10.1007/s11071-008-9432-5

[9] Shi, J., Wei, Q., & Zhao, Y. (2007). Analysis of dynamic response of the high-speed EMS maglev vehicle/guideway coupling system with random irregularity. *Vehicle System Dynamics*, *45*(12), 1077–1095. https://doi.org/10.1080/00423110601178441

[10] Yau, J. D. (2010). Interaction response of maglev masses moving on a suspended beam shaken by horizontal ground motion. *Journal of Sound and Vibration*, *329*(2), 171–188. https://doi.org/10.1016/j.jsv.2009.08.038

[11] Wang, B., Zhang, Y., Xia, C., Li, Y., & Gong, J. (2022). Dynamic analysis of high-speed maglev train-bridge system with fuzzy proportional-integral-derivative control. *Journal of Low Frequency Noise Vibration and Active Control*, *41*(1), 374–386. https://doi.org/10.1177/14613484211029133

[12] Sinha, P. K., & Pechev, A. N. (1999). Model reference adaptive control of a maglev system with stable maximum descent criterion. *Automatica*, *35*(8), 1457–1465. https://doi.org/10.1016/S0005-1098(99)00040-0

[13] Jeong, J.-H., Ha, C.-W., Lim, J., & Choi, J.-Y. (2016). Analysis and control of the electromagnetic coupling effect of the levitation and guidance systems for a semi-high-speed MAGLEV using a magnetic equivalent circuit. *IEEE Transactions on Magnetics*, *52*(7). https://doi.org/10.1109/TMAG.2015.2506681

[14] Sun, Y., Xu, J., Wu, H., Lin, G., & Mumtaz, S. (2021). Deep learning based semi-supervised control for vertical security of maglev vehicle with guaranteed bounded airgap. *IEEE Transactions on Intelligent Transportation Systems*, *22*(7), 4431–42. https://doi.org/10.1109/TITS.2020.3045319

[15] Teklu, E. A. & Abdissa, C. M. (2023). Genetic algorithm tuned super twisting sliding mode controller for suspension of maglev train with flexible track. *IEEE Access*, *11*, 30955–30969. https://doi.org/10.1109/ACCESS.2023.3262416

[16] Bosera, A. S., Olana, F. D., Merga, C. & Gutole, S. T. (2022). Adaptive PSO based gain optimization of sliding mode control for position tracking control of magnetic levitation systems, *2022 International Conference on Information and Communication Technology for Development for Africa (ICT4DA)*, Bahir Dar, Ethiopia, 157–162. https://doi.org/10.1109/ICT4DA56482.2022.9971197

[17] Yu, P. C., Li, J., & Zhou, D. F. (2016). A performance assessment method for suspension control system of maglev train. *2016 Chinese Control and Decision Conference (CCDC)*, Yinchuan, China. https://doi.org/3509.10.1109/CCDC.2016.7531590

[18] Ding, J. F., Liang, S. & Long, Z. Q. (2019). Research on performance evaluation method of levitation control system for maglev train. *Proceedings - 2019 Chinese Automation Congress (CAC)*, Hangzhou, China, 628–633. https://doi.org/10.1109/CAC48633.2019.8997517

[19] Song, Y. F., Ni, F., Lin, G. B., & Xu, J. Q. (2020). Data-driven control loop performance evaluation of electromagnetic levitation systems. *2020 Chinese Automation Congress (CAC)*, Shanghai, China, 502. https://doi.org/10.1109/CAC51589.2020.9326993

[20] Liu, X., Zhu, P., Li, Z., Fan, W. & Li, X. (2022). Performance evaluation of suspension control system based on minimum variance. *2022 5th International Conference on Data Science and Information Technology (DSIT)*, Shanghai, China, 1–5. https://doi.org/10.1109/DSIT55514.2022.9943976

[21] Xu, Y., Long, Z., Zhao, Z., Zhai, M., & Wang, Z. (2022). Real-time stability performance monitoring and evaluation of maglev trains' levitation system: A data-driven approach. *IEEE Transactions on Intelligent Transportation Systems*, *23*(3), 1912–1923. https://doi.org/10.1109/TITS.2020.3029905

[22] Liu, X., Zhu, P., Li, Z., Liang, S., & Li, X. (2022). Performance evaluation of maglev train suspension system based on data drive. *2022 34th Chinese Control and Decision Conference (CCDC)*, Piscataway, NJ, USA, 1763–1768. https://doi.org/10.1109/CCDC55256.2022.10034332

[23] Hurst, H. E. (1951). Long-term storage capacity of reservoirs. *Transactions of the American Society of Civil Engineers*, *116*, 770–799. https://doi.org/10.1061/taceat.0006518

[24] Mandelbrot, B. B., & Wallis, J. R. (1969). Robustness of the rescaled range R/S in the measurement of noncyclic long run statistical dependence. *Water Resources Research*, *5*(5), 967–988. https://doi.org/10.1029/WR005i005p00967

[25] Chen, Z., Hu, K., Carpena, P., Bernaola-Galvan, P., Stanley, H. E., & Ivanov, P. C. (2004). Effect of nonlinear filters on detrended fluctuation analysis. *Physical Review E - Statistical, Nonlinear, and Soft Matter Physics*, *71*(1). https://doi.org/10.1103/PhysRevE.71.011104

[26] Srinivasan, B., Spinner, T., & Rengaswamy, R. (2012). Control loop performance assessment using detrended fluctuation analysis (DFA). *Automatica*, *48*(7), 1359–1363. https://doi.org/10.1016/j.automatica.2012.04.003

[27] Das, L., Srinivasan, B., & Rengaswamy, R. (2016). Multivariate control loop performance assessment with Hurst exponent and Mahalanobis distance. *IEEE Transactions on Control Systems Technology*, *24*(3), 1067–1074. https://doi.org/10.1109/TCST.2015.2468087

[28] Domański, P. D., & Ławryńczuk, M. (2017). Assessment of predictive control performance using fractal measures. *Nonlinear Dynamics*, *89*(2), 773–790. https://doi.org/10.1007/s11071-017-3484-3

[29] Domański, P. D. (2019). Control quality assessment using fractal persistence measures. *Isa Transactions*, *90*, 226–234. https://doi.org/10.1016/j.isatra.2019.01.008

[30] Khosroshahi, M., & Poshtan, J. (2021). Data-driven performance assessment of multivariable control loops using a modified Hurst exponent-based index. *Proceedings of the Institution of Mechanical Engineers, Part I: Journal of Systems and Control Engineering*, *235*(6), 769–780. https://doi.org/10.1177/0959651820966523

[31] Liu, Z., Long, Z., & Li, X. (2015). *Maglev Trains*. Springer Berlin, Heidelberg. https://doi.org/10.1007/978-3-662-45673-6

[32] Jing, H., & Yang, L. (2017). Research on Window Function Selection in Phase Estimation of Digital Signal. *5th International Conference on Frontiers of Manufacturing Science and Measuring Technology (FMSMT)*, Taiyuan, People's Republic of China, *130*, 1162–1165. https://doi.org/10.2991/fmsmt-17.2017.228

[33] Wang, J. Y., Gu, C. C., & Liu, K. C. (2022). Anomaly electricity detection method based on entropy weight method and isolated forest algorithm. *Frontiers in Energy Research*, *10*. https://doi.org/10.3389/fenrg.2022.984473

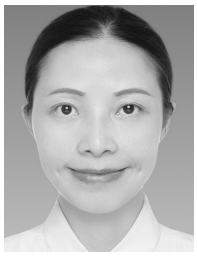

Fei Ni received the M.Sc. degree in applied mathematics from Northwestern Polytechnical University, Xi'an, China in 2010, and the Ph.D. degree in natural sciences from RWTH Aachen University, Aachen, Germany, in 2015. From 2015 to 2017, she was a Postdoctoral Researcher with the Eindhoven University of Technology, Eindhoven, the Netherlands. She is currently with the National Maglev Transportation Engineering R&D Center, Tongji University, Shanghai, China. Her research interests include uncertainty quantification, intelligent control & performance evaluation of the maglev train.

Lijun Rong received the B.Sc. in mechanical manufacturing automation from Hunan University, Changsha, China in 1996, and his M.Sc. in mechatronics from the same university, in 1999. He is currently working for the National Maglev Transportation Engineering R&D Center, Tongji University, Shanghai, China. He is also working toward his Ph.D. degree from Southwest Jiaotong University, Chengdu, China. His research interests include levitation control technology of the maglev train and coupling vibration between the maglev train and track.

Metrol. Meas. Syst., Vol. 31 (2024), No. 1, pp. 115–133
DOI: 10.24425/mms.2024.148539

Yawen Dai received the B.Sc. degree in vehicle engineering from Tongji University, Shanghai, China in 2022. She is currently working toward M.Sc. at the National Maglev Transportation Engineering R&D Center, Tongji University, Shanghai, China. Her research interest is performance evaluation of the maglev train.

Junqi Xu received the Ph.D. degree from Southwest Jiaotong University, China, in 2020. He is currently a Research Fellow and the Deputy Director of the National Maglev Transportation Engineering R&D Center at Tongji University. He has authored more than 60 academic papers, obtained more than 20 granted patents, and participated in setting 6 standards. He has won 2 first class prizes and 2 second class prizes of provincial and ministerial scientific and technological progress, 1 second class prize for technological invention. His current research interests include the maglev train and intelligent control technology.

Qinghua Zheng received the Dipl. Math. and Dr. rer. nat. degrees from the University of Hamburg, Germany, in 1984 and 1987, respectively. From 1984 to 1988, he was a Research Assistant with the Institute of Applied Mathematics, University of Hamburg. From 1988 to 2001, he was a Senior Expert, the Project Leader, a Senior Principal Scientist with the Siemens Research and Development Center in Munich and Princeton. Since 2001, he has been with ThyssenKrupp Transrapid GmbH, Munich. In 2014, he become a Guest Professor with Tongji University, Shanghai, China. His research interests include nonlinear dynamics and control, numerical algorithms, and data analysis.